Direct observation of ballistic and drift carrier transport regimes in InAs nanowires

X. Zhou, S. A. Dayeh, D. Aplin, D. Wang, and E. T. Yu[a)]
Department of Electrical and Computer Engineering, University of California, San Diego, La Jolla, California 92093-0407 and Materials Science Program, University of California, San Diego, La Jolla, California 92093-0407

(Received 17 February 2006; accepted 7 June 2006; published online 2 August 2006)

Conductive atomic force microscopy has been used to characterize distance-dependent electron transport behavior in InAs nanowires grown by metal-organic chemical vapor deposition. Using a conducting diamond-coated tip as a local electrical probe in an atomic force microscope, the resistance of the InAs nanowire has been measured as a function of electron transport distance within the nanowire. Two regimes of transport behavior are observed: for distances of ~200 nm or less, resistance independent of electron transport distance, indicative of ballistic electron transport, is observed; for greater distances, the resistance is observed to increase linearly with distance, as expected for conventional drift transport. These observations are in very good qualitative accord with the Landauer formalism for mesoscopic carrier transport, and the resistance values derived from these measurements are in good quantitative agreement with carrier concentrations and mobilities determined in separate experiments. These results provide direct information concerning distances over which ballistic transport occurs in InAs nanowires as well as demonstrating the ability of the scanning probe techniques employed to characterize nanoscale transport characteristics in semiconductor nanowire structures. © *2006 American Institute of Physics*.
[DOI: 10.1063/1.2236589]

Quasi-one-dimensional systems such as semiconductor nanowires and nanotubes are of outstanding current interest as building blocks for nanoscale electronic and optoelectronic devices.[1–4] Among the semiconductor materials that have been explored for nanowires, InAs is particularly intriguing[5,6] due to its small electron effective mass, correspondingly high bulk electron mobility, and inherent surface accumulation of electrons. Indeed, recent studies of InAs nanowire-based field-effect transistor structures have demonstrated electron mobilities in excess of 6000 $cm^2/V\,s$—the highest carrier mobility observed in a semiconductor nanowire to date and an indication of their promise for high-speed device applications.[7]

To achieve effective control over and optimization of the characteristics and performance of such devices, direct experimental characterization of structure, electronic properties, and carrier transport behavior is essential. However, conventional macroscopic electrical measurements of nanowire characteristics provide only limited, and often somewhat indirect, information concerning their detailed behavior at the nanoscale. Scanning probe measurements of local electrical properties offer the possibility of direct experimental characterization of electronic structure and carrier transport properties with spatial resolution typically in the range of tens of nanometers.[8,9]

We have used conductive atomic force microscopy (cAFM) to probe the electronic properties of semiconductor nanowire devices at the nanoscale. Using a conducting scanning probe tip as a local electrical contact, we have measured two-terminal resistance as a function of electron transport length within an InAs nanowire. For transport lengths of ~200 nm or less, length-independent resistance indicative of ballistic transport behavior is observed. For greater transport lengths, the resistance is found to increase approximately linearly with length, as expected for conventional drift transport.

The InAs nanowires employed in these studies were grown by metal-organic chemical vapor deposition using colloidal Au nanoparticles for nucleation on thermally oxidized Si substrates. The nanowires were unintentionally doped *n* type, and for each growth nanowire diameters typically in the range of 50–100 nm. Following sonication to release the nanowires into solution, the nanowires were deposited onto a 600 nm SiO_2 layer produced by thermal oxidation on a n^+ Si (001) substrate. Electron beam lithography followed by 15 nm Ti/85 nm Al metallization and a standard lift-off process was used to create Ohmic contacts to the randomly positioned nanowires. The well-known phenomenon of Fermi-level pinning above the conduction-band edge of InAs (Ref. 10) enabled ready formation of low-resistance Ohmic contacts to the InAs nanowires. Figure 1(a) shows a scanning electron microscope (SEM) image of a 50 nm diameter InAs nanowire structure with two Ohmic contacts. Current-voltage characteristics for these nanowire structures are typically highly linear, as shown in Fig. 1(b), confirming the high quality of the Ohmic contacts, with average electron mobilities in excess of 3000 $cm^2/V\,s$.[7]

Scanned probe measurements were performed using a Digital Instruments/Veeco Nanoscope III Multimode atomic force microscope to which a current preamplifier was attached to enable cAFM measurements.[11] The experimental geometry is shown schematically in Fig. 2. A diamond-coated scanning probe tip served as a positionable electrical contact to the InAs nanowire, with the macroscopic Ohmic contact fabricated lithographically serving as the second contact to the nanowire for a two-terminal measurement of elec-

[a)]Electronic mail: ety@ece.ucsd.edu

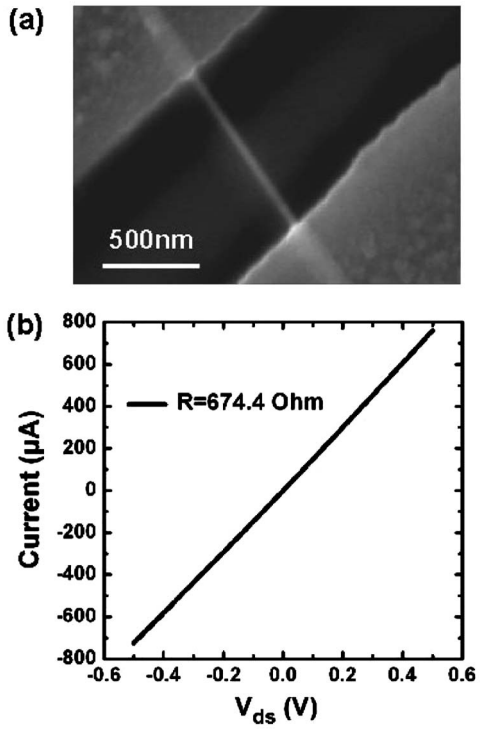

FIG. 1. (a) SEM image of InAs nanowire grown by metal-organic chemical vapor deposition (MOCVD) and subsequently deposited on SiO_2, with Ti/Al Ohmic contacts patterned by electron-beam lithography. (b) Representative two-terminal current-voltage characteristic for such a device.

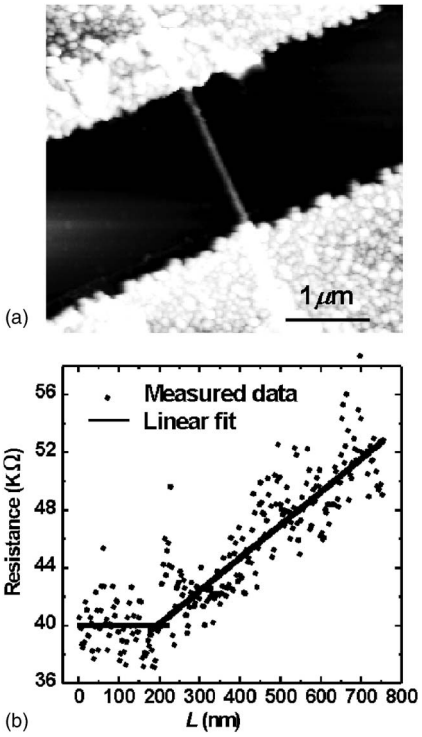

FIG. 3. (a) AFM topograph of InAs nanowire and Ti/Al Ohmic contacts. (b) Resistance measured by cAFM as a function of tip-contact distance L (symbols), with linear fits for the ballistic transport regime (L below ~200 nm), for which resistance is independent of L, and the drift transport regime (L above ~200 nm), for which resistance increases linearly with L.

trical current flow through the nanowire. A dc bias voltage V_{sd} was applied between the macroscopic contact and the conducting probe tip, and the resulting current was measured as a function of distance L between the probe tip and the edge of the contact. The second macroscopic Ohmic contact shown in Fig. 2 remained floating, and therefore did not contribute to the current flow observed in these measurements.

Figure 3(a) shows an AFM topograph of the device, consisting of a 75 nm diameter InAs nanowire with two Ohmic contacts fabricated as described previously, employed in these studies. Current images acquired at fixed V_{sd} simultaneously with the topograph reveal a trend of constant to decreasing current I with increasing tip-contact distance L, suggesting that the nanowire resistance contributes significantly to the total device resistance, and as expected generally increases with transport distance within the nanowire. The detailed behavior of current flow as a function of electron transport distance within the nanowire can be elucidated by extracting the total resistance $R \equiv V_{sd}/I$ as a function of electron transport distance L, as shown in Fig. 3(b). The data in Fig. 3(b) were derived from cAFM images by averaging current measured at several points over a distance of ~20 nm normal to the nanowire axis, and clearly reveal two distinct regimes of behavior. For electron transport distances below approximately 200 nm, R is observed to be independent of L, while for larger distances, R increases approximately linearly with L. Linear fits to these two regions are also shown in Fig. 3(b), and yield a constant contribution to the device resistance of ~40 kΩ and a length-dependent contribution of ~23 kΩ/μm.

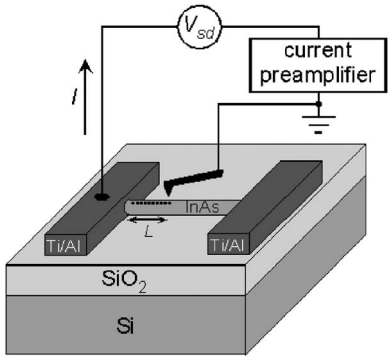

FIG. 2. Schematic diagram of experimental probe tip and sample geometry and electrical measurement configuration. Current I is measured for fixed bias voltage V_{sd} as a function of tip-contact distance L, with the probe tip forming a positionable contact to the nanowire in a two-terminal device measurement.

These results may be interpreted as follows. The total resistance of the tip-nanowire-Ohmic contact structure can be written, adapting the well-known Landauer formalism, as[12]

$$R = R_{\text{drift}} + \frac{h}{2e^2 M} + R_{\text{tip-nanowire}} + R_{\text{series}}, \tag{1}$$

where R_{drift} is the contribution due to scattering during drift transport in the nanowire, $h/2e^2M$ is the contact resistance to the nanowire, accounting for the difference in current carrying modes between the contacts and nanowire, with M being the number of propagating electron modes in the nanowire, $R_{\text{tip-nanowire}}$ is the additional resistance between the probe tip and the nanowire, and R_{series} is the parasitic series resistance associated with external wiring and wire bonds and the patterned metal electrodes. Of these contributions, only R_{drift}

depends directly on L; therefore, any dependence observed of R on L should constitute primarily a dependence of the nanowire resistance on L.

The observation of a range of tip-contact distances for which R is independent of L suggests that electron transport over these distances within the nanowire is primarily ballistic. In this regime, the observed resistance of $\sim 40\ \mathrm{k}\Omega$ is dominated by the remaining terms in Eq. (1). Since the contact resistance of a single-mode conductor is $h/2e^2 = 12.9\ \mathrm{k}\Omega$, this result suggests that parasitic series resistances or nonidealities, e.g., thin insulating layers, at the contacts contribute significantly but not overwhelmingly to the observed resistance. As carrier scattering becomes more prominent for longer electron transport distances, R_{drift}, the contribution to the total resistance from carrier scattering in the nanowire associated with conventional drift transport, should increase from zero linearly with L. This is in very good accord with the experimental observations shown in Fig. 3(b).

Furthermore, a very simple quantitative estimate of the wire resistivity expected on the basis of wire dimensions, expected carrier concentrations, and mobility measured in similar InAs nanowire structures yields good quantitative agreement with the experimentally measured value of $23\ \mathrm{k}\Omega/\mu\mathrm{m}$. Specifically, the familiar expressions for resistivity and resistance adapted to account for the presence of electrons both at the InAs surface and within the bulk material region yield

$$R_{\mathrm{drift}}/L \approx \frac{1}{q[\pi(r_{\mathrm{wire}} - r_{\mathrm{surf}})^2 n_{\mathrm{bulk}}\mu_{\mathrm{bulk}} + 2\pi r_{\mathrm{wire}} n_{\mathrm{surf}}\mu_{\mathrm{surf}}]}, \tag{2}$$

where q is the fundamental electronic charge magnitude, r_{wire} is the nanowire radius, r_{surf} is the thickness of the InAs electron surface accumulation layer, n_{bulk} is the bulk volume electron concentration, n_{surf} is the surface electron concentration, μ_{bulk} is the bulk electron mobility, and μ_{surf} is the surface electron mobility. Given a nanowire diameter of 75 nm, estimating the bulk electron concentration to be $5 \times 10^{16}\ \mathrm{cm}^{-3}$, the surface electron accumulation layer thickness to be 10 nm, and the surface electron concentration to be $0.5 \times 10^{11}\ \mathrm{cm}^{-2}$,[13,14] and using the measured electron mobility in very similar InAs nanowires of $\sim 2000\ \mathrm{cm}^2/\mathrm{V\,s}$, which most likely reflects the relatively low mobility of electrons at the InAs surface compared to that in the bulk, as well as possible structural defects within the wire,[7] we obtain a resistance per unit length for the InAs nanowire of $24\ \mathrm{k}\Omega/\mu\mathrm{m}$—very close to the experimental value of $23\ \mathrm{k}\Omega/\mu\mathrm{m}$ derived from the data of Fig. 3(b). Very similar mobilities have recently been reported in planar[15] ($\sim 2000\ \mathrm{cm}^2/\mathrm{V\,s}$) and vertical[16] ($\sim 3000\ \mathrm{cm}^2/\mathrm{V\,s}$) InAs nanowire transistors, further supporting the validity of the mobility value used in this calculation.

It should be noted that despite the very good agreement observed between the measured InAs nanowire resistance and that calculated using the simple approach described above, the measured resistance may be somewhat larger than that associated specifically with electron transport within the nanowire. Because the nanowire resistance increases with tip-contact distance L, the potential drop across the nanowire increases with L as well. As a result, the potential drop across the nanowire contacts will decrease as L increases for measurements performed at fixed bias voltage V_{sd}. This could be of particular importance for the tip-nanowire contact, which is more likely to contain contamination or insulating interfacial layers that yield nonideal Ohmic contact behavior. For such a nonideal Ohmic contact, the resistance $R_{\mathrm{tip\text{-}sample}}$ in Eq. (1) would increase with decreasing voltage across the contact, resulting in an additional contribution to R as L increases in the measurements presented in Fig. 3(b). While this subtlety may influence the quantitative determination of the nanowire resistance per unit length, however, it does not impact the observation of ballistic transport within the nanowire nor the determination of the length scales over which electron transport within the nanowire is predominantly ballistic in nature. In summary, we have used cAFM to characterize electron transport behavior in InAs nanowires, and have observed clear evidence of electrical current conduction dominated by either ballistic (at short distances) or drift (at longer distances) motion of electrons, with the transition between ballistic- and drift-dominated transports occurring at electron transport distances of ~ 200 nm. The resulting dependence of resistance of the InAs nanowire device on electron transport distance within the nanowire is in very good qualitative accord with the Landauer formalism for mesoscopic carrier transport, and the values of resistance derived from our measurements are in good quantitative agreement with those estimated from the nanowire dimensions combined with carrier concentrations and mobilities estimated or determined in separate experiments.

Part of this work was supported by the National Science Foundation (DMR 0405851 and ECS 0506902).

[1] Y. Cui, Z. Zhong, D. Wang, W. U. Wang, and C. M. Lieber, Nano Lett. **3**, 149 (2003).
[2] D. D. D. Ma, C. S. Lee, F. C. K. Au, S. Y. Tong, and S. T. Lee, Science **299**, 1874 (2003).
[3] L. Samuelson, M. T. Bjork, K. Deppert, M. Larssonb, B. J. Ohlssonc, N. Paneva, T. Ohshima, and N. Yokoyama, Physica E (Amsterdam) **21**, 560 (2004).
[4] A. Bachtold, P. Hadley, T. Nakanishi, and C. Dekker, Science **294**, 1317 (2001).
[5] Y. Doh, J. A. van Dam, A. L. Roest, E. P. A. M. Bakkers, L. P. Kouwenhoven, and S. D. Franceschi, Science **309**, 272 (2005).
[6] C. Thelander, T. Martensson, M. T. Bjork, B. J. Ohlsson, M. W. Larsson, L. R. Wallenberg, and L. Samuelson, Appl. Phys. Lett. **83**, 2052 (2003).
[7] S. Dayeh, D. Aplin, X. Zhou, P. K. L. Yu, E. T. Yu, and D. Wang, *47th Electronic Materials Conference*, Santa Barbara, CA (2005).
[8] Y. Yaish, J. Y. Park, S. Rosenblatt, V. Sazonova, M. Brink, and P. L. McEuen, Phys. Rev. Lett. **92**, 046001 (2004).
[9] X. Zhou, E. T. Yu, D. Florescu, J. C. Ramer, D. S. Lee, and E. A. Armour, Appl. Phys. Lett. **85**, 407 (2004).
[10] C. A. Mead and W. G. Spitzer, Phys. Rev. Lett. **10**, 471 (1963).
[11] E. J. Miller, D. M. Schaadt, E. T. Yu, C. Poblenz, C. Elsass, and J. S. Speck, J. Appl. Phys. **91**, 9821 (2002).
[12] S. Datta, *Electronic Transport in Mesoscopic Systems* (Cambridge University Press, Cambridge, 1995).
[13] E. Yamaguchi and M. Minakata, Appl. Phys. Lett. **43**, 965 (1983).
[14] Y. Tsuji, T. Mochizuki, and T. Okamato, Appl. Phys. Lett. **87**, 062103 (2005).
[15] Y. J. Doh, J. A. van Dam, A. L. Roest, E. P. A. M. Bakkers, L. P. Kouwenhoven, and S. De Franceschi, Science **309**, 272 (2006).
[16] T. Bryllert, L. Wernersson, L. E. Fröberg, and L. Samuelson, IEEE Electron Device Lett. **27**, 323 (2006).